PNAS
www.pnas.org

Supplementary Information for

Stress Increases in Exopher-mediated Neuronal Extrusion Require Lipid Biosynthesis, FGF, and EGF RAS/MAPK Signaling

Jason F. Cooper[1], Ryan J. Guasp[1], Meghan Lee Arnold[1], Barth D. Grant[1,2], Monica Driscoll[1,3]

Department of Molecular Biology and Biochemistry

[1]Rutgers University, Piscataway, NJ USA, Rutgers University
[2]Rutgers Center for Lipid Research
[3]*Corresponding Author:* Monica Driscoll

Email Address: driscoll@biology.rutgers.edu

Tel: (848-445-7182)

This PDF file includes:

Expanded Methods
Supplementary text
Figures S1 to S4 (not allowed for Brief Reports)
Tables S1 (not allowed for Brief Reports)

Expanded Materials and Methods

Genetics

Generation of strains. We generated genetic strains using standard techniques in the field. We crossed ZB4065 males to mutant animals, and males resulting from the mating were back-crossed to the homozygous deletion mutant a minimum of three times. We confirmed the parental genotype by PCR for large deletion mutants or by sequencing for point mutants. We determined homozygosity of transgenic fluorescent loci by confirming 100% animal fluorescence in three sequential generations.

Strains used in this study were:

ZB4065 *bzIs166* [P$_{mec-4}$mCherry1] II, also referred to as mCherryAg2

ZB5160 *bzIs166* [P$_{mec-4}$mCherry1] II*; hsf-1(sy441)* I

ZB5161 *bzIs166* [P$_{mec-4}$mCherry1] II; *kgb-1(um3)* IV

ZB5162 *bzIs166* [P$_{mec-4}$mCherry1] II; *skn-1(zj15)* IV

ZB5163 *bzIs166* [P$_{mec-4}$mCherry1] II; *jun-1(gk551)* II

ZB5164 *bzIs166* [P$_{mec-4}$mCherry1] II; *hif-1(ia4)* V

ZB5165 *bzIs166* [P$_{mec-4}$mCherry1] II; *daf-16(mu86)* I

ZB5166 *bz166* [P$_{mec-4}$mCherry1] II; *hlh-30(tm1978)* IV

ZB5186 *bzIs166* [P$_{mec-4}$mCherry1] II; *let-60(n1046)* IV

SK4005 *zdIs5*[P$_{mec-4}$GFP]

BY250 *vtIs7*[P$_{dat-1}$GFP]

ZB4599 *let-23(sa62*) II; *bzIs166* [P$_{mec-4}$mCherry1] II

ZB5184 *bzIs166* [P$_{mec-4}$mCherry1] II; *sid-1(qt9)* V; *sqIs71* [P$_{rgef-1}$GFP; P$_{rgef-1}$*sid-1*;pBS]

ZB5185 *bzIs166* [P$_{mec-4}$mCherry1] II; *sid-1(qt9)* V; *alxIs6* [P$_{vha-6}$*sid-1*::sl2::GFP]

ZB5020 *bzIs166* [P$_{mec-4}$mCherry1] II; *mkcSi13* [P$_{sun-1}$*rde-1*::*sun-1* 3'UTR + *unc-119*(+)] II; *rde-1(mkc36)* V

ZB5173 *bzIs166* [P$_{mec-4}$mCherry1] II; *sid-1(qt9)* V; *bzIs153* [P$_{myo-2}$*sid-1*]

ZB5172 *bzIs166* [P$_{mec-4}$mCherry1] II; *rde-1(mkc36)* V; *mfIs70*[P$_{lin-31}$*rde-1*; P$_{myo-2}$GFP]

ZB5298 *bzIs166* [P$_{mec-4}$mCherry1] II; *sid-1(qt9)* V*; bzSi33* [P$_{myo-2}$ *sid-1*; P$_{myo-2}$GFP]

ZB5299 *bzIs166* [P$_{mec-4}$mCherry1] II; *sid-1(qt9)* V; *bzSi13* [P$_{hyp-7}$*sid-1*; P$_{myo-2}$GFP]

ZB5300 *bzIs166* [P$_{mec-4}$mCherry1] II; *sid-1(qt9)* V; *uthIs237* [P$_{myo-3}$tomato; P$_{myo-3}$*sid-1*]

ZB5301 *bzIs166* [P$_{mec-4}$mCherry1] II; *let-23(sa62)* II; *bzIs155* [P$_{myo-2}$GFP] (promoter-less control)

ZB5302 *bzIs166* [P$_{mec-4}$mCherry1] II; *bzIs152* [P$_{unc-119}$*let-23(sa62);* P$_{myo-2}$GFP]

ZB5303 *bzIs166* [P$_{mec-4}$mCherry1] II; *bzIs151* [P$_{myo-3}$*let-23(sa62);* P$_{myo-2}$GFP]

ZB5304 *bzIs166* [P$_{mec-4}$mCherry1] II; *bzIs153* [P$_{vha-6}$*let-23(sa62);* P$_{myo-2}$GFP]

ZB5171 *bzSi39* [P$_{mec-7}$HttQ74::mNG]; *bzSi34* [P$_{mec-7}$mScarlet::IFD-1]

Stress Studies

Heat stress experiments. For studies of chronic heat stress we collected ZB4065 animals at the L4 stage of development on 50 mm diameter OP50-seeded NGM media plates. We then isolated 50 animals every 8 h starting at Ad1, paralyzed animals in 5 mM levamisole, and counted exophers using a ringed microscope slide on a Kramer high-power dissecting microscope on days 1, 2, 3, and 4 of adulthood. To evaluate chronic heat stress beginning at the egg stage, we plated 25 animals and allowed egg laying overnight. We placed the resulting progeny in incubators preset to 15, 20, or 25 °C. For studies of acute heat stress, we cultured Ad1 ZB4065 animals on OP50-seeded NGM plates at 4, 15, 20, 30, or 37 °C for 6-hours. We collected the animals, paralyzed them in 5 mM levamisole, and scored them for exophers using ringed cytology slides on a Kramer FBS10 pseudo-stereo fluorescence dissecting microscope for observation.

Fasting stress experiments. We grew age-synchronized animals on OP50-seeded NGM plates and collected animals in M9, washed them 3x, and deposited on them upon unseeded NGM plates for 6 h. We then collected the animals, paralyzed them in 5 mM

levamisole, and scored the animals at the desired age for ALMR exophers using ringed cytology slides on a Kramer fluorescence dissecting microscope.

Oxidative stress experiments. We determined exopher sensitivity of ZB4065 animals to acute oxidative stress using juglone (Sigma, St. Louis, MO, USA), paraquat (methyl viologen, Sigma), and rotenone (MP Bio). We transferred Ad1 animals to freshly prepared NGM plates containing juglone, paraquat or rotenone at molarities indicated in the Results section and assessed exopher production 6-h post-exposure. We measured exophers under chronic oxidative stress through exposure to plates containing paraquat or rotenone (at indicated molarities) beginning at Ad1. We measured exopher production every 24 h until the indicated day of adulthood.

Osmotic stress. We determined sensitivity to acute osmotic stress by moving Ad1 worms to NGM plates containing 500 mM concentrations of NaCl, sucrose, glucose, or sorbitol, and scoring exophers after 6 h of exposure. We measured sensitivity to chronic osmotic stress by moving Ad1 worms to OP50-seeded NGM plates containing 250 mM concentrations of NaCl, sucrose, glucose, or sorbitol. We scored exophers using ringed cytology slides on a fluorescent Kramer dissecting microscope every 24 h until Ad4.

Anoxic/Hypoxic Stress. We subjected animals to anoxic stress by transferring Ad1 worms into an anaerobic chamber (GasPak, BD) on OP50 seeded or unseeded NGM plates. We introduced hypoxia using an adjustable hypoxia C-174 chamber (Biospherix). We washed animals raised under atmospheric conditions using standard M9 and placed into the C-174 chamber adjusted for 0.1% oxygen for 6 h. We scored exposed animals using ringed cytology slides on a fluorescent Kramer dissecting microscope.

RNAi screening

We administered RNAi through feeding animals bacteria that expressed specific dsRNA using standard methods and available libraries [28, 73]. In brief, we selected *E. coli* HT115 strains that expressed double-stranded RNA (dsRNA) of the *C. elegans* genes of interest [29, 74] and used NGM agar with tetracycline and carbenicillin to select for the L4440 RNAi plasmid; we used IPTG (Isopropyl β-D-1-thiogalactopyranoside) to strongly activate T7 polymerase expression and transcription of the dsRNA within each bacterial culture. We seeded IPTG plates with the transformed bacterial culture expressing dsRNA targeting the gene of interest overnight. Some of the genes of interest led to developmental failure, so to avoid exposing animals to lifelong knockdown, we moved animals to the RNAi plates at the L4 stage and scored for exophers on the second day of adulthood. We scored 50 animals per trial where noted in Figure Legends. Supplemental Table 1 lists genes that we tested, which we sequenced to confirm molecular identities.

Exopher scoring and statistical analysis

We identified and quantified exophers as documented in detail in previous publications [4, 10]. To determine whether a genetic or chemical intervention modulates the rate of exopher production, we consider exopher detection as an “exopher-event” for a given neuron. In other words, exopher events are scored as binary (yes/no)—either an exopher is present or it is not. An exopher event can include the observation of a single exopher near a soma or multiple exophers in the vicinity. ALMR neurons produce the most baseline exophers in the strains described herein and therefore we focus on ALMR scores for exopher quantitation from touch receptor neurons. For trials comparing exopher production in one mutant or treatment to control, we used the Cochran-Mantel-Haenszel (CMH) statistical test. For multiple trials involving one or two mutants or

treatments compared to control, the CMH test is also appropriate for *p*-value determination.

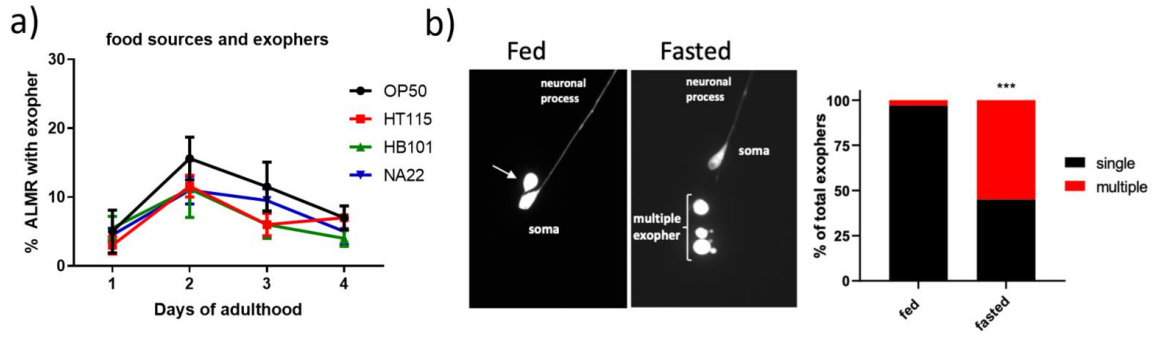

Supplemental Figure 1: Food source does not significantly change exopher production levels. However, fasting, a potent inducer of neuronal exophers, modulates both exopher number and morphology.

a) *E. coli* strain does not affect exophergenesis under basal feeding conditions. We grew strain mCherryAg2 on *E. coli* OP50, 20 °C until the adolescent L4 stage, splitting animals to plates growing *E. coli* strains HT115 (red line), HB101 (green line), or NA22 (blue line), evaluating exophers on Ad1-4; 4x trials, 50 animals per trial, Cochran–Mantel–Haenszel (CMH) statistics.

b) Exopher events in fasted animals exhibit high incidences of multiple exophers from a single ALMR neuron. Left, representative images of ALMR exophers in strain mCherryAg2; right is quantitation. 6 h fasting executed at Ad1 commonly induces multiple exophers while multiples are not frequent in fed animals. 20 animals per condition, Fisher's Exact test ***p<0.001.

Discussion. Whereas exophers produced by well-fed control populations are visualized predominantly as single ejected structures, fasted animals routinely exhibit multiple exophers. Examples of multiple exophers are rare in control animals (less than 5%), but are observed in 40-60% of fasting-induced exopher events. A multiple-exopher event might be the consequence of repeated exopher production by an individual neuron, or alternatively, a single extruded exopher might be more rapidly split into fragments within the receiving hypodermal tissue. We favor the former model because in the case of fasting, we can often observe multiple exophers still connected to the soma by filamentous tunneling nanotube-like structures. These filaments are hypothesized to be generated in individual extrusion events (see Figure 1a). Alternatively, increased degradation into multiple fragments within the hypodermal compartment post-extrusion would be consistent with a measured increase in autophagy that accompanies food deprivation. Either way, our observations raise the possibility that certain facets of exopher production and/or degradation might be different when fasting signals are activated as compared to when they are not.

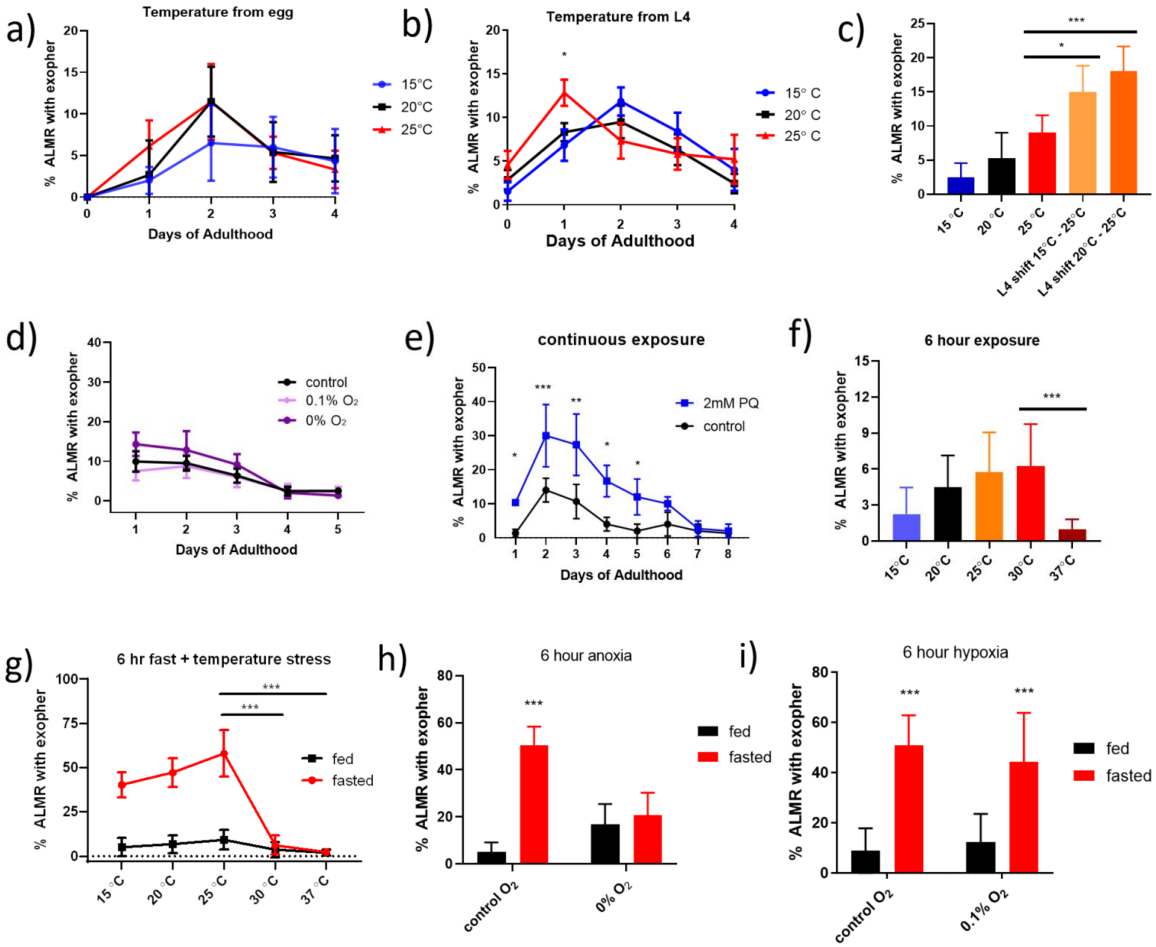

Supplemental Figure 2: Environmental stresses have a differential impact upon exopher production.

For all panels bars are SEM, ***p<0.001, **p<0.01 *p<0.05, CMH statistics.

a) Animals reared at 15 °C, 20 °C, and 25 °C throughout their lives show little difference in early adult exopher levels. We grew strain mCherryAg2 continuously at the temperatures indicated from the egg stage and scored ALMR exophers on the days of adult life indicated. Because animals develop at slightly different rates at different temperatures, Ad1 was defined as 24 h after the identification of the L4 vulval crescent phenotype. We find no significant differences in exopher levels under the different growth temperatures, 50 animals per trial, 4x trials.

b) Animals reared at 20 °C and *temperature shifted* to 15 °C, 20 °C, or 25 °C at the L4 stage reveal an earlier temporal peak at 25 °C. We reared strain mCherryAg2 at 20 °C to the L4 stage and split and distributed animals to the indicated temperatures over adult lifespan, sampling on the indicated days. We quantitated exopher production from ALMR. 4x trials, 50 animals per trial for each condition on each day of sampling.

c) Transient shift to an *increased* temperature increases exophergenesis. Animals were raised continuously at 15 °C, 20 °C, or 25 °C concurrently with animals shifted from 15 °C to 25 °C at the L4 stage and animals shifted from 20 °C to 25 °C at the L4 stage. Exophers were scored for exophers on Ad2. We find that animals that undergo a shift to an increased temperature have increased exopher production. 4x trials, 50 animals per trial.

d) Limiting oxygen availability does not markedly enhance exopher production. Indicated are ALMR counts for acute anoxia (0% O_2) or hypoxia (0.1% O_2) delivered in a nitrogen displacement chamber for 6 h on Ad1. 5x trials, 50 animals per trial.

e) Continuous exposure to 2 mM paraquat increases exopher levels from Ad1 to Ad4. We grew mCherryAg2 animals at 20 °C, transferred to 2 mM paraquat plates at Ad1, scoring for ALMR exophers each day until Ad8, 3x trials, 50 animals per trial.

f) High temperature exposure can suppress exopher production. We raised mCherryAg2 animals at 20 °C and then exposed animals to the range of temperatures indicated for 6 h, scoring ALMR exophers shortly thereafter. Note that 30 °C and 37 °C are temperatures used to introduce heat stress and can ultimately kill *C. elegans* under long exposures. Exopher production at 37 °C is significantly lower as compared to 30 °C, 4x trials, 50 animals per trial.

g) Combined food withdrawal and temperature stress can suppress exopher induction under conditions that individually induce high exopher levels. We fasted Ad1 mCherryAg2 animals for 6 h at temperatures indicated and scored for ALMR exophers shortly thereafter. 3x trials, 50 animals per trial. Note the difference in exopher levels for 30 °C animals alone vs. when combined with food limitation at 30 °C.

h) Anoxic 0% oxygen conditions blunt fasting-induced exopher production. We fasted Ad1 mCherryAg2 animals within an anoxia chamber at 0% oxygen for 6 hours and scored for ALMR exophers shortly thereafter, 5x trials, 50 animals per trial.

i) Hypoxic 0.1% oxygen conditions DO NOT blunt fasting-induced exopher production. We fasted Ad1 mCherryAg2 animals within a hypoxia chamber calibrated to maintain 0.1% oxygen for 6 h and scored for ALMR exophers shortly thereafter, 5x trials, 50 animals per trial.

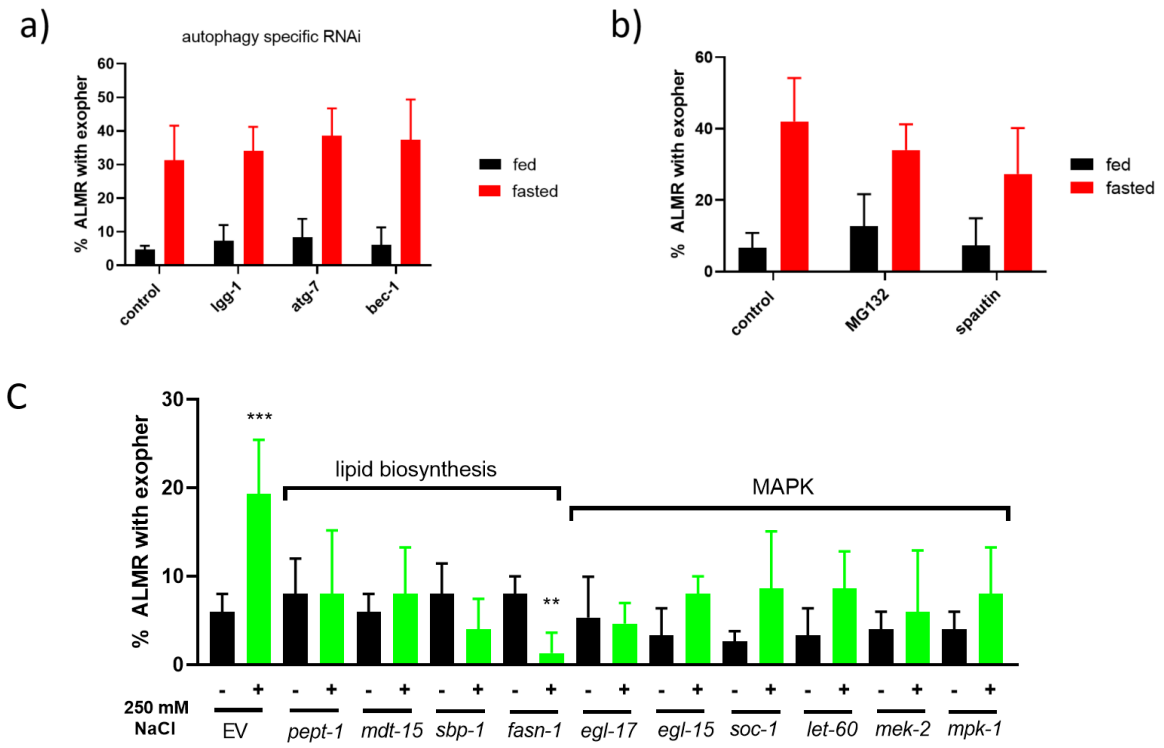

Supplemental Figure 3: Suppression of lipid biosynthesis and MAPK signaling can also suppress osmotic stress-induced exophergenesis, whereas disruption of autophagy or the proteasome do not prevent fasting induced exophers.

For all panels, bars are SEM, ***p<0.001, **p<0.01 *p<0.05, CMH statistics. Feeding RNAi was initiated at the L4 larval stage and continued until Ad2.

a) RNAi targeted against autophagy-specific genes fails to influence the fasting induced exopher response. Animals were exposed to RNAi from the L4 stage until Ad2. We fasted Ad2 mCherryAg2 animals for 6 h and scored for ALMR exophers shortly thereafter, 3x trials, 50 animals per trial.

b) Pharmacological disruption of neither proteasomal degradation (MG132) nor autophagy (spautin) significantly influences fasting-induced exophergenesis. Animals were exposed to each compound from the egg stage until Ad2. We fasted Ad2 mCherryAg2 animals for 6 h and scored for ALMR exophers shortly thereafter, 3x trials, 50 animals per trial.

c) Lipid biosynthesis and MAPK signaling suppress osmotic stress-induced exophergenesis. Animals were concurrently exposed to 250 mM NaCl stress and RNAi against the indicated gene beginning from L4 until Ad2. Genes that were able to suppress fasting-induced exophergenesis were also able to suppress exophergenesis in a hyperosmotic environment. 3x trials, 50 animals per trial.

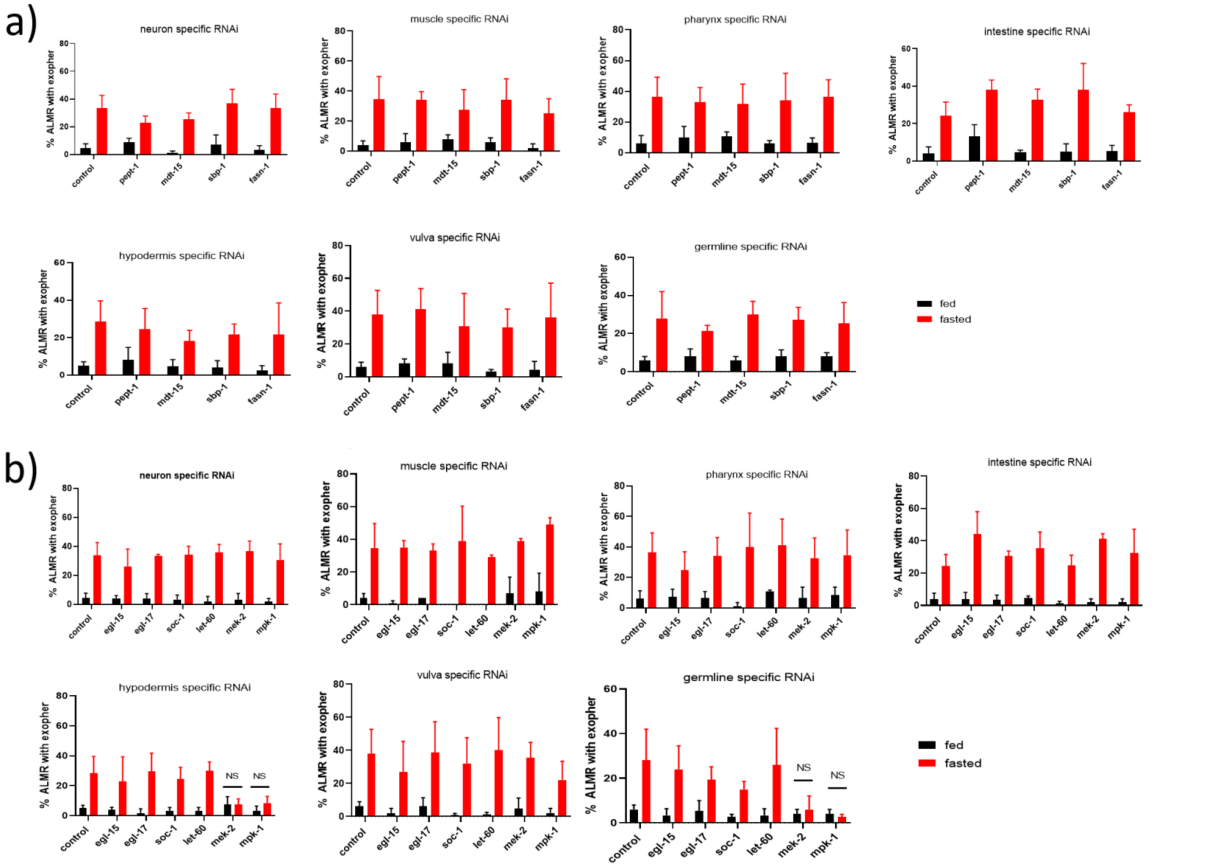
a)
neuron specific RNAi
muscle specific RNAi
pharynx specific RNAi
intestine specific RNAi
hypodermis specific RNAi
vulva specific RNAi
germline specific RNAi
% ALMR with exopher
control
pept-1
mdt-15
sbp-1
fasn-1
fed
fasted
b)
egl-15
egl-17
soc-1
let-60
mek-2
mpk-1
NS
c)
tissue specific RNAi
***
lin-3
germline
neuron
intestine
hypodermis
muscle
vulva
d)
mex-3 RNAi
% animals surviving by adult day 1
e)
rab-10 RNAi
% animals with vacuolation
EV
rab-10
f)
% animals moving
unc-13 RNAi
unc-14 RNAi
control
P intestine::sid-1
P neuron::sid-1
g)
lin-3
let-23
egl-15
soc-1
Tissue-specific gene expression (YA)
log2 TPM
Germline
Neurons
Muscle
Hypod.
Intest.

Supplemental Figure 4: RNAi targeting MAPK signaling and lipid signaling genes tested in seven strains sensitized to RNAi exclusively in a single tissue implicate germline-derived EGF and hypodermis in fasting stress induction of exophers.

For all panels, bars are SEM, ***p<0.001, **p<0.01 *p<0.05, CMH statistics. Feeding RNAi was initiated at the L4 larval stage and continued until Ad2. For all panels the same ten genes comprising lipid signaling and MAPK signaling were knocked down using RNAi in strains sensitized to RNAi in only one tissue.

a) RNAi targeting genes involved in lipid synthesis/signaling did not suppress fasting-induced exopher production when RNAi was sensitized only within a single tissue. RNAi knockdown of the indicted gene beginning at the L4 stage in the mCherryAg2 strain, 6-h fast followed by exopher assay on Ad2, control is empty vector RNAi. 3x trials, 50 animals per trial.

b) RNAi targeting of crucial nodes of MAPK signaling suppress fasting induced exopher production when RNAi targeting is restricted to the germline or to the hypodermis. RNAi knockdown of the indicated gene beginning at the L4 stage in the mCherryAg2 strain, 6-h fast followed by exopher assay on Ad2, control is empty vector RNAi. *mek-2* and *mpk-1* were found to suppress fasting-induced exophergenesis when RNAi targeting is restricted to the germline (ZB5172) or the hypodermis (ZB5299), 3x trials, 50 animals per trial.

c) RNAi knockdown of EGF *lin-3* in the germline alone is sufficient to suppress fasting-induced exophergenesis. RNAi against EV or *lin-3* was initiated at the L4 stage utilizing strains that are sensitive to RNAi exclusively in the denoted tissue. A 6-h fast was followed by exopher quantification at Ad2. 3x replicates, 50 animals per trial.

d) General RNAi quality control targeting *mex-3*. RNAi knockdown of *mex-3* prevents the development of mCherryAg2 progeny, but not progeny derived from strains that are only sensitive to RNAi within neurons (*bzIs166* [P_{mec-4}mCherry1]; *sid-1(qt9)* V; *sqIs71*[P_{rgef-1}GFP; P_{rgef-1}*sid-*1;pBS]) or intestinal cells (*bzIs166*[P_{mec-4}mCherry1]; *sid-1(qt9)* V; *alxIs6*[P_{vha-6}*sid-1*::sl2::GFP]). We placed 10 Ad1 animals per RNAi plate for each condition and allowed them to lay eggs overnight. Their progeny were allowed to develop for 72 h before we quantitated survival.

e) Intestine-specific RNAi quality control targeting *rab-10*. RNAi knockdown of *rab-10* causes the development intestinal vacuolization in mCherryAg2 animals, but the effect blunted in animals sensitive to RNAi specifically in the germline (*bzIs166* [P_{mec-4}mCherry1]; *sid-1(qt9)* V; *sqIs71* [P_{rgef-1}GFP; P_{rgef-1}*sid-1*;pBS]). We placed 10 Ad1 animals per RNAi plate for each condition and allowed them to lay eggs overnight. Their progeny were allowed to develop for 72 h before they were imaged for a vacuolization phenotype.

f) Neuron-specific RNAi quality control targeting *unc-13* and *unc-14*. RNAi knockdown of *unc-13* and *unc-14* causes a decrease in motility in mCherryAg2 animals. The effect is exacerbated in a strain only sensitive to RNAi within neurons ([P_{mec-4}mCherry1]; *sid-1(qt9)* V; *sqIs71*[P_{rgef-1}GFP; P_{rgef-1}*sid-1*;pBS]), but the effect is blunted in a strain that is not sensitive to RNAi ([P_{mec-4}mCherry1]; *sid-1(qt9)* V; *alxIs6*[P_{vha-6}*sid-1*::sl2::GFP]). We placed 10 Ad1 animals per RNAi plate for each condition and allowed them to lay eggs overnight. Their progeny were allowed to develop for 72 h before evaluation. Motility in progeny was scored by quantitating the percentage of animals that began to move when perturbed with a gentle touch from a probe.

g) Expression data of FGF and EGF MAPK signaling components determined by RegAtlas. The Ahringer laboratory generously maintains an open source tool, RegAtlas, part of which is database of expression data for *C. elegans* that can be assessed by tissue. RegAtlas is derived from data initially presented in [43]. The y-axis shows transcripts per million (TPM) as assessed on Ad1. EGF component *lin-3* is expressed predominantly in the germline, while *let-23* is mainly found in the neurons and intestine. On the other hand, FGF component *egl-15* is found mostly in the hypodermis and *soc-1* in the intestine and the hypodermis.

Supplemental Discussion

Summary of tissue-specific pathway perturbations suggest initial models for distributed tissue activity in fasting-induced exopher production.

Lipid synthesis is likely to be contributed by multiple tissues and act upstream of MAPK signaling. Because RNAi knockdown of each required lipid synthesis gene (*pept-1, mdt-15, sbp-1, fasn-1*) in each specific tissue tested (neurons, muscle, pharynx, intestine, hypodermis, germline, vulva) fails to block fasting-induced responses, but whole animal RNAi (apart from neurons) can disrupt fasting-induced induction of exophers, we infer that lipid synthesis genes may be expressed in multiple tissues to produce a signal, or an essential lipid, required for fasting-induced exophergenesis. Knockdown of any one of these genes in a single tissue is not sufficient to eliminate the fasting-induced exopher elevation response. The lipid synthesis requirement is most likely to act upstream of MAPK activation since RNAi knockdown of members of the lipid synthesis group in *let-60(gf)* and in the neuronal *let-23(gf)* strain does not alter the neuronal *let-23(gf)* phenotype of elevated exopher levels even when continuously fed. A caveat in the epistasis studies is that neuronal disruption is not likely to be effective in the aforementioned test. If there were a critical lipid biosynthesis requirement in neurons, it would most likely be missed. Since neuron-specific knockdown of the lipid biosynthesis group does not change fasting stress elevation of exophers, our data do not support a probable essential role for lipid synthesis genes in neurons. We cannot rule out ineffective neuronal RNAi knockdown of the targeted genes in our study; control neuronal RNAi studies indicate functional knockdown of test neuronal genes *unc-13* and *unc-14* (Supplemental Figure 4d-f), with levels likely reduced but expression not fully eliminated.

Germline EGF *lin-3*, MAPKK *mek-2* and MAPK *mpk-1* can influence neuronal exopher outcomes. EGF/*lin-3* expression is required in the germline for fasting-induced exopher elevation, as are EGF downstream pathway MAPK genes *mek-2* and *mpk-1* (Supplemental Figure 4b). FGFR/*egl-15* and FGF pathway-specific *soc-1* do not appear required in the germline. The EGF pathway might function in an autocrine-like pathway that establishes a positive feedback loop for EGF expression; but multiple roles of MAPK signaling in the germline are known (41).

A MAPK pathway in the hypodermis might influence exopher levels. It is interesting that our tissue-specific knockdown data also indicate a requirement for MAPKK *mek-2* and MAPK *mpk-1* in the hypodermis. Although we cannot rule out that the hyp7 promoter we used for hypodermal specific *sid-1* rescue might also be unexpectedly expressed in the germline, the different outcome for EGF *lin-3* RNAi suggests that explanation is unlikely. It is notable that the exopher-producing touch neuron that we measure for exopher production (ALMR) is fully embedded in the hypodermis; the hypodermis is the tissue that receives the exopher and attempts to digest its contents (4). FGF signaling pathway components are known to be highly expressed in hypodermis (46), (see Supplemental Figure 4g; https://ahringerlab.com/RegAtlas/), suggesting an FGF pathway in the neighboring cell, which receives the exophers, might influence the exopher extrusion in the neuron which it surrounds. Since hypodermal specific RNAi-directed against upstream FGFR/*egl-15* and *soc-1* did not suffice to disrupt the fasting-induced elevation of exophers, our data suggest that additional tissues contribute FGF-dependent signaling that influences this process. Our data indicate that such FGF signaling transpires upstream of EGF pathway signaling in neurons. However, given the caveats applicable to general and tissue-specific RNAi, especially as concern negative outcomes, establishing details of this model awaits extensive cell- and tissue-specific rescue experiments.

Neuronal EGFR activation can elevate exopher formation in the presence of food. Our data show that activation of EGFR in neurons using transgenic expression of *let-23(gf)* can elevate exopher levels in the presence of food, suggesting that a neuronal EGF pathway could suffice to influence the process. There is a possibility that neuronal EGFR/*let-23(gf)* expression creates an artificial situation. For example, if neurons are ectopically induced for the pathway, the downstream outcome, such as production of a neuropeptide, could be sufficient to boost exophergenesis, even though under normal circumstances activation transpires via another tissue (apart from muscle and intestine, which we rule out); evidence for a requirement for EGF pathway specific EGFR/*let-23* in neurons (or other tissues) is currently lacking. If the EGF pathway were activated in neurons by fasting-induced signaling, EGFR might act directly in the touch neurons to elevate exophergenesis or might generate a signal from another neuron that acts non-autonomously to promote touch neuron exopher production. Our data suggest that it is most likely that EGF signaling acts downstream of FGF signaling and may impact neurons.

Potential for cross-talk and pathway complexities. It should be noted that our data suggest additional MAPK activities that might modulate exophergenesis levels. One characterized stress and longevity pathway involves MLK-1/MAPKKK, SHC-1 adaptor, MEK-1/MAPKK and KGB-1/MAPK, which can intersect with both the insulin signaling pathway and heavy metal stress response [66, 67]. Our RNAi knockdown of *shc-1, mlk-1*, and *kgb-1* did not disrupt fasting induced exopher elevation, suggesting that this MAPK module is not engaged to influence exopher production under food limitation stress. Our data do, however, suggest a role for *mek-1*/MAPKK in fasting-induced elevation of exophers. *mek-1*/MKK7 functions in the stress response to heavy metals copper and cadmium, as well as starvation [68]. Heavy metal resistance requires adaptor homolog *shc-1/* p52Shc [66], but our RNAi data suggest that *shc-1* is dispensable for exopher modulation, and thus, if RNAi targeting was effective, the MEK-1 contribution may be distinct from the heavy metal response. MEK-1 can interact with MEK-2 in cells [69] so it is possible that MEK-1 functions as a required MAPKK in the FGF pathway we describe.

Gene	Sequence	Gene	Sequence	Gene	Sequence
aak-1	PAR2.3	*fos-1*	F29G9.4	*par-5*	M117.2
aak-2	T01C8.1	*ftt-2*	F52D10.3	*pept-1*	K04E7.2
aakg-4	T01B6.3	*icl-1*	C05E4.9	*pha-4*	F38A6.1
abl-1	M79.1	*ins-3*	ZK75.3	*pmk-1*	B0218.3
age-1	B0334.8	*ins-4*	ZK75.1	*pod-2*	W09B6.1
akt-1	C12D8.10	*ist-1*	C54D1.3	*pqm-1*	F40F8.7
akt-2	F28H6.1	*kgb-1*	T07A9.3	*prg-1*	D2030.6
alh-6	F56D12.1	*kri-1*	ZK265.1	*prmt-1*	Y113G7B.17
bar-1	C54D1.6	*ksr-1*	F13B9.5	*ptp-2**	F59G1.5
ced-9	T07C4.8	*ksr-2*	F58D5.4	*rheb-1*	F54C8.5
cep-1	F52B5.5	*lam-3*	F59G1.5	*rict-1*	F29C12.3
cst-1	F14H12.4	*lea-1*	K08H10.1	*rle-1*	M142.6
daf-12	F11A1.3	*let-23*	ZK1067.1	*rsks-1*	Y47D3A.16
daf-15	C10C5.6	*let-363*	B0261.2	*sbp-1*	Y47D3B.7
daf-18	T07A9.6	*let-60*	ZK792.6	*sem-5*	C14F5.5
daf-28	Y116F11B.1	*lin-1*	C37F5.1	*shc-1*	F54A5.3
daf-7	B0412.2	*lin-3**	F36H1.4	*sir-2.1*	R11A8.4
daf-9	T13C5.1	*lin-31*	K10G6.1	*skn-1*	T19E7.2
dbl-1	T25F10.2	*lin-35*	C32F10.2	*smk-1*	F41E6.4
din-1	F07A11.6	*lipl-2*	F46B6.8	*sos-1**	T28F12.3
egl-15	F58A3.2	*lipl-4*	K04A8.5	*sup-17*	F38G1.2
egl-17	F38G1.2	*lrp-1*	F56D1.4	*svh-1**	C07G1.1
elo-5	F41H10.7	*mdt-15*	R12B2.5	*svh-2*	T14E8.1
elo-6	F41H10.8	*mek-1*	K08A8.1	*tax-6*	C02F4.2
elt-2	C33D3.1	*mek-2**	Y54E10BL.6	*tiar-1*	C18A3.5
elt-3	K02B9.4	*mgl-1*	ZC506.4	*tps-1*	ZK54.2
eor-1	R11E3.6	*mlk-1*	K11D12.10	*tps-2*	F19H8.1
fasn-1	F32H2.5	*mpk-1*	F43C1.2	*ucp-4*	K07B1.3
fat-2	W02A2.1	*mxl-3*	F46G10.6	*unc-43*	K11E8.1
fat-5	W06D12.3	*nhr-45*	F16H11.5	*vab-1*	M03A1.1
fat-6	VZK822L.1	*nhr-49*	K10C3.6	*vhp-1*	F08B1.1
fat-7	F10D2.9	*nsy-1*	F28B12.3	*vrk-1*	F28B12.3

Supplemental Table 1: List of all genes tested at least once in the fasting-pathway RNAi screen.

We listed gene names and identifier sequences for each gene we tested in our initial screen for genes operative in the fasting-induced exopher response. All genes came from the *C. elegans* RNAi Collection (Ahringer library) unless noted by an asterisk, in which case the gene came from the *C. elegans* ORFeome (Vidal library). Genes that were considered positive hits were then sequenced and replicated. Negative outcomes cannot be considered to rule out any gene on this list as single RNAi results are not definitive.